

# VISUALIZATION OF BRAIN WHITE MATTER TRACTS USING HEAVILY T2-WEIGHTED THREE-DIMENSIONAL FLUID-ATTENUATED INVERSION-RECOVERY MAGNETIC RESONANCE IMAGING

MASAHIRO YAMAZAKI, SHINJI NAGANAWA, KIMINORI BOKURA, and HISASHI KAWAI

*Department of Radiology, Nagoya University Graduate School of Medicine, Nagoya, Japan*

## ABSTRACT

The purpose of this study was to elucidate which white matter (WM)-tracts are visualized on heavily T2-weighted three-dimensional fluid-attenuated inversion-recovery (hT2w-3D-FLAIR) images. Records of seven patients who underwent hT2w-3D-FLAIR and diffusion tensor imaging (DTI) of the head at 3 Tesla were analyzed. Two neuroradiologists determined WM-tracts visualized on hT2w-3D-FLAIR and identified anatomical points through which they ran. A third neuroradiologist determined the WM-tracts running through those points on DTI. Correspondence between hT2w-3D-FLAIR and DTI WM-tracts was used to confirm technique validity. As a result, the corticospinal tract (CST), medial lemniscus (ML), and superior cerebellar peduncle (SCP) were visualized as high intensity on hT2w-3D-FLAIR and ran through the following points: CST, 20 mm lateral from the lateral margin of the third ventricle at the thalamic level; ML, 6 mm anterior to the anterior margin of the fourth ventricle at the trigeminal nerve level; and SCP, just lateral to the fourth ventricle at the trigeminal nerve level. The third neuroradiologist determined that the WM-tracts ran through those points on DTI in all patients. Consequently, WM-tracts determined on hT2w-3D-FLAIR and DTI completely corresponded. In conclusion, the CST, ML, and SCP were visualized as high intensity on hT2w-3D-FLAIR. This technique is a potentially supplemental DTI neurographic modality.

Key Words: Magnetic resonance imaging, 3D-imaging, Heavily T2-weighted three-dimensional fluid-attenuated inversion-recovery (hT2w-3D-FLAIR), Brain, White matter tracts

## INTRODUCTION

Heavily T2-weighted three-dimensional fluid-attenuated inversion-recovery (hT2w-3D-FLAIR) imaging of the inner ear for 4 h after intravenous gadolinium injection has been reported to separately visualize perilymph and endolymph fluid, and to identify the presence of endolymphatic hydrops in patients with Ménière's disease.<sup>1, 2)</sup> The central nervous system, including the brainstem, is also included in these images. It is noticeable that some white matter (WM)-tracts are visualized as high-intensity regions with strong contrast between the surrounding brain

---

Received: April 14, 2014; accepted: May 19, 2014

Corresponding author: Masahiro Yamazaki, MD

Department of Radiology, Nagoya University Graduate School of Medicine, 65 Tsurumai-cho, Showa-ku, Nagoya 466-8550, Japan.

Telephone: +81-52-7442327, Fax: +81-52-7442335, E-mail: yamazaki@med.nagoya-u.ac.jp

parenchyma. From this perspective, we thought that hT2w-3D-FLAIR might supplement diffusion tensor imaging (DTI) neurographic modality if particular WM-tracts can be visualized. Consequently, the purpose of the present study was to elucidate which WM-tracts were visualized on hT2w-3D-FLAIR, and to confirm that those WM-tracts corresponded to those visualized on DTI to affirm the validity of the imaging technique.

## MATERIALS AND METHODS

### *Study population*

The records of seven consecutive adult patients (1 male, 6 female; aged 22–69 years; mean age, 48.1 years) who underwent hT2w-3D-FLAIR and DTI of the head at our hospital in January 2012 were analyzed retrospectively. All patients were clinically suspected of having Ménière's disease, and they underwent magnetic resonance imaging (MRI) for detailed examination to determine whether endolymphatic hydrops was present. All patients underwent intravenous administration of a single-dose (0.2 ml (0.1 mmol)/kg) body weight) of gadolinium-diethylenetriamine pentaacetic acid-bis (methylamide) (Gd-DTPA-BMA) (Omniscan, Daiichi Sankyo Co., Ltd., Tokyo, Japan) and underwent MRI for 4 h after intravenous gadolinium injection. This delay was chosen because a delay of 4 h between intravenous gadolinium injection and MRI has been reported to be optimal to allow wide distribution of gadolinium in the lymphatic space of the labyrinth in healthy participants.<sup>3)</sup> Written informed consent was obtained from all patients and the study was approved by the Ethics Review Committee of our institution.

### *MRI protocol*

All scans were performed using a 3 Tesla MRI (Magnetom Verio; Siemens AG, Erlangen, Germany) with a receive-only, 32-channel, phased-array coil. The hT2w-3D-FLAIR and DTI for anatomical reference were obtained at the same visit.

The parameters for the hT2w-3D-FLAIR were as follows: sampling perfection with application-optimized contrast using different flip angle evolution (SPACE)-based sequences with frequency-selective fat-suppression pre-pulse; repetition time (TR), 9000 msec; echo time (TE), 544 msec; inversion time (TI), 2250 msec; initial refocusing flip angle, 180°, rapidly decreased to constant flip angle, 120° for the turbo spin-echo (TSE) refocusing echo train in SPACE sequence; echo train length, 173; matrix size, 322 × 384; 104 axial, 1-mm-thick slices covering from the body of the lateral ventricle level to the upper cervical spinal cord level including the labyrinth with a 150 × 180 mm field of view (FOV); generalized autocalibrating partially parallel acquisition (GRAPPA)<sup>4)</sup> acceleration factor, 2; voxel size, 0.5 × 0.5 × 1.0 mm; number of excitations (NEX), 4; scan time, 14 min 26 sec; readout bandwidth, 434 Hz/pixel; and echo spacing, 5.56 msec.

The parameters for DTI were as follows: less distortion readout-segmented multi-shot EPI (RESOLVE)-based sequence<sup>5)</sup>; TR, 4500 msec; TE, 76 msec; refocusing flip angle, 180°; b-factors, 0 and 700 sec/mm<sup>2</sup>, 10 directions; number of k-space segmentations, 9; matrix size, 192 × 192; 26 axial, 3-mm-thick slices, 0.3-mm slice gap; FOV, 180 × 180 mm; GRAPPA acceleration factor, 2; voxel size, 0.9 × 0.9 × 3.0 mm; NEX, 1; scan time, 9 min 11 sec; and readout bandwidth, 592 Hz/pixel. The trace images, apparent-diffusion-coefficient (ADC) map, fractional-anisotropy (FA) map, and color map were automatically produced on the scanner console. In the present color assignment, green represents anterior-posterior, red represents lateral-lateral, and blue represents superior-inferior orientations.

### *Imaging evaluation*

The coronal and sagittal hT2w-3D-FLAIR (7-mm slice thickness, 1-mm slice gap) images were reconstructed from axial images. The reconstructed slice thickness of 7 mm was determined by two neuroradiologists by agreement prior to the experiment, considering the signal to noise ratio and the visibility of the continuity of the WM-tracts. The same two neuroradiologists observed the hT2w-3D-FLAIR in three directions and determined that the WM-tracts were visualized as high-intensity areas with consensual decision making for all patients. In addition, the two neuroradiologists also determined the anatomical points that those WM-tracts ran through on the axial hT2w-3D-FLAIR images in all patients. The third neuroradiologist then determined the WM-tracts running through those anatomical points on axial DTI color maps without reference to the hT2w-3D-FLAIR images. The correspondence of the detected WM-tracts between hT2w-3D-FLAIR and DTI was assessed as affirmation that those WM-tracts were identical structures. In addition, the existence of motion artifacts was also assessed visually at the same time as the WM-tracts analysis.

## RESULTS

No image of any patients showed motion artifacts. The two neuroradiologists determined that the corticospinal tract (CST), medial lemniscus (ML), and superior cerebellar peduncle (SCP) were visualized as high-intensity areas on the hT2w-3D-FLAIR in all patients (Fig. 1). In addition, those WM-tracts ran through the following anatomical points on the axial hT2w-3D-FLAIR in all patients (Fig. 2 **A, B**): CST, 20 mm lateral from the lateral margin of the third ventricle at the thalamic level (point A); ML, 6 mm anterior to the anterior margin of the fourth ventricle at the trigeminal nerve level (point B); and SCP, just lateral to the fourth ventricle at the trigeminal nerve level (point C). The third neuroradiologist determined that the following WM-tracts ran through those anatomical points on axial DTI color maps of all patients without referring to hT2w-3D-FLAIR (Fig. 2 **C, D**): (point A) CST; (point B) ML; and (point C) SCP. The WM-tracts determined from hT2w-3D-FLAIR and DTI thus completely corresponded and were considered to be identical structures.

## DISCUSSION

The present study revealed that the CST, ML and SCP were visualized on high-resolution hT2w-3D-FLAIR images. These results are considered reliable because the WM-tracts determined on hT2w-3D-FLAIR completely corresponded to those visualized on DTI using less distortion readout-segmented multi-shot EPI.

Previous studies have reported that the WM-tracts such as the CST are visualized as high-intensity regions on two-dimensional (2D)-spin-echo (SE)-FLAIR or 2D-SE-T2-weighted imaging.<sup>6, 7</sup> In those reports, the high signals of particular WM-tracts were thought to arise from structural features of WM-tracts such as unmyelinated or sparsely myelinated fibers within the tracts<sup>6</sup> or the presence of large fibers with thick myelin sheaths.<sup>7</sup> In addition, recent reports suggest that it is unlikely that the visualization of WM-tracts on 3D-FLAIR using varying flip angles is related to noticeable inherent diffusion sensitivity.<sup>8</sup> In the present study, the CST, ML, and SCP were visualized on hT2w-3D-FLAIR, although the other WM-tracts, such as the middle cerebellar peduncle, were not clearly visualized. Considering the descriptions in the above-mentioned literature, the results of the present study are likely due to T2 differences

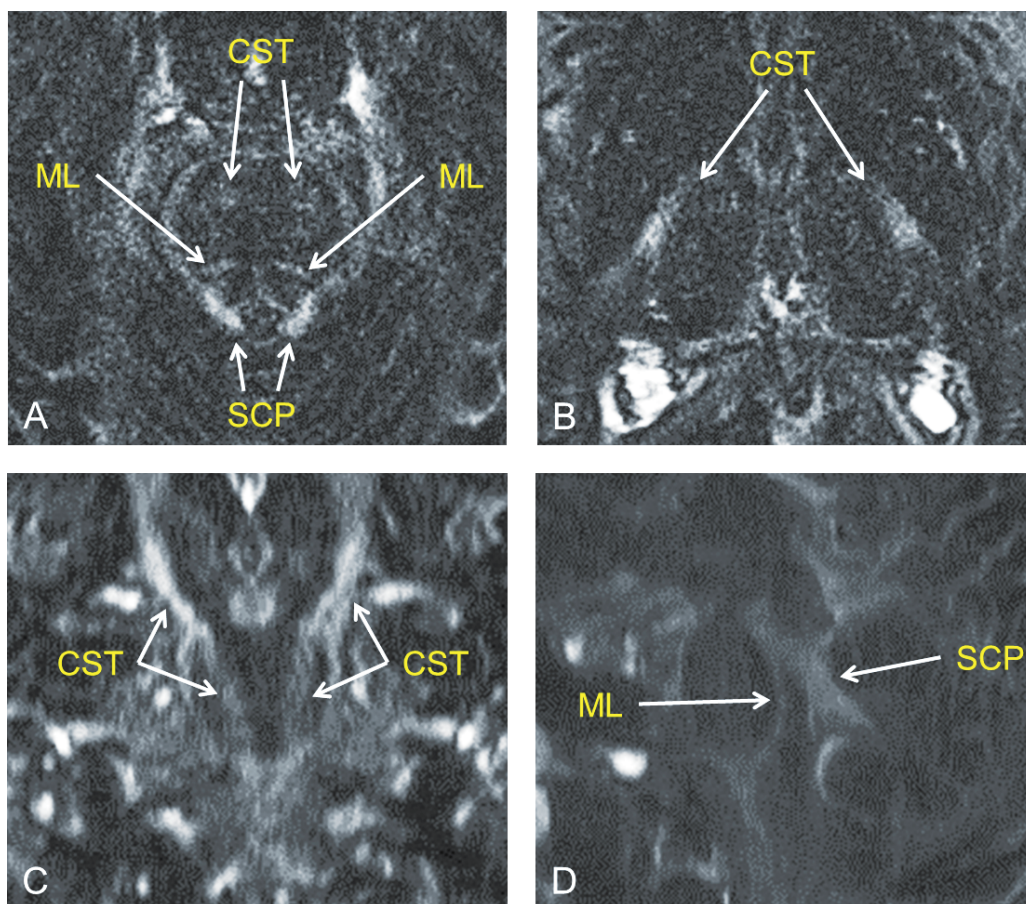


**Fig. 1** Axial (A: the pontine level, B: the thalamic level), coronal (C: the pontine level), and sagittal (D: the median level) heavily T2-weighted three-dimensional fluid-attenuated inversion-recovery (hT2w-3D-FLAIR) images of a single patient are presented. The corticospinal tract (CST), medial lemniscus (ML), and superior cerebellar peduncle (SCP) are visualized as high-intensity areas.

attributable to the structural features of particular WM-tracts rather than the effect of diffusion related to the direction of the nerve fibers.

At the present moment, the methodologies of visualization or analysis of WM-tracts are generally based on diffusion-weighted imaging (DWI) or echo planar imaging (EPI) techniques.<sup>9-12)</sup> However, DTI (which applies DWI) is limited regarding the analysis of nerve crossings. In addition, EPI is affected strongly by magnetic susceptibility, and less distortion readout-segmented multi-shot EPI techniques (such as RESOLVE-based sequences) have the dilemma of scan time prolongation. hT2w-3D-FLAIR is a high-resolution and isotropic 3D-sequence. Therefore, hT2w-3D-FLAIR has the possibility of providing supplementary information to DTI, because the present study revealed that particular WM-tracts such as the CST, ML, and SCP could be visualized on hT2w-3D-FLAIR. Consequently, a comparison study on hT2w-3D-FLAIR between normal and abnormal groups, such as progressive supranuclear palsy or amyotrophic lateral sclerosis, may provide supplementary information about the diagnosis of those diseases.

The superiority of visualization of WM-tracts of the brain stem on 3D-FLAIR compared with

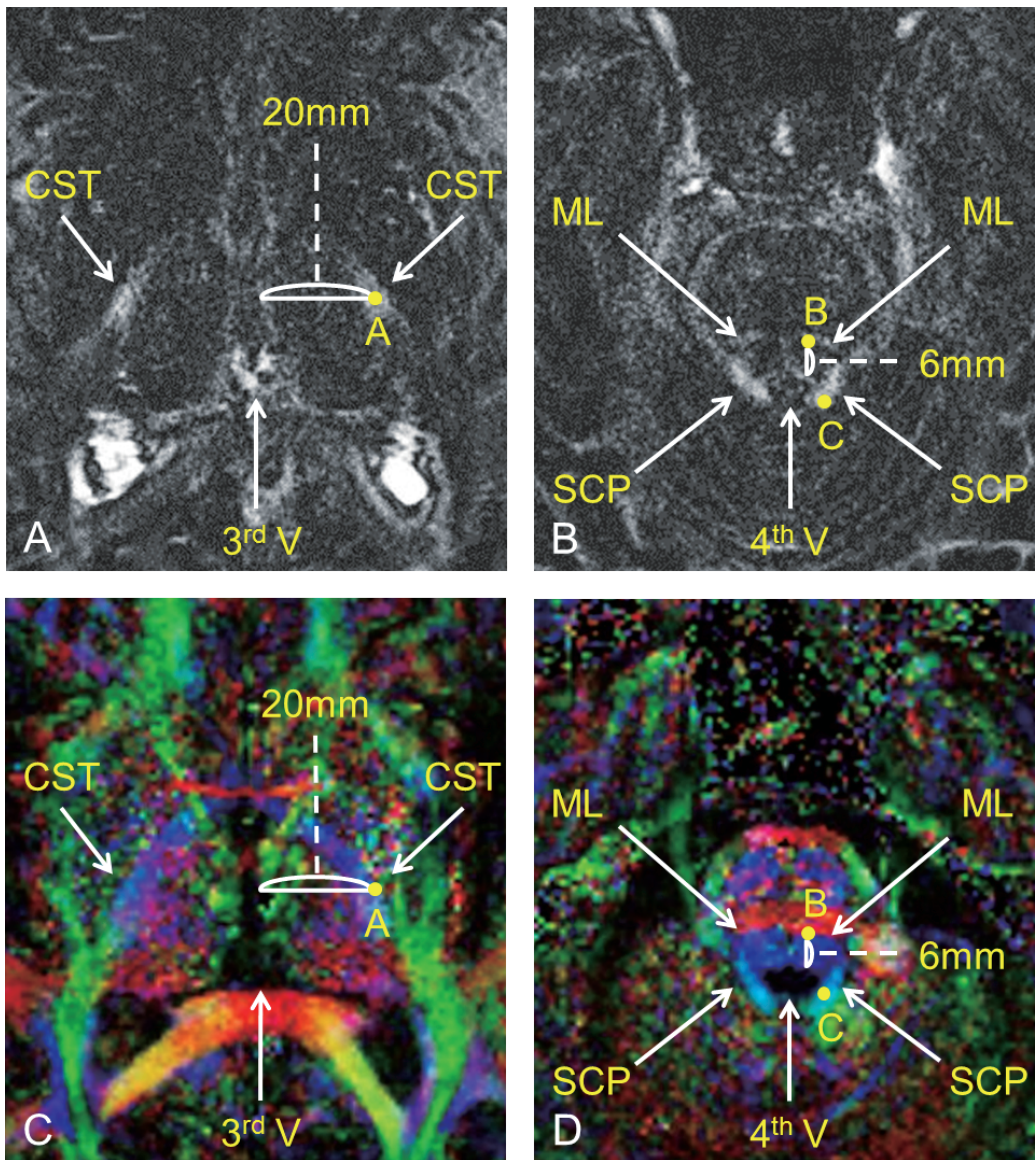


**Fig. 2** Axial heavily T2-weighted three-dimensional fluid-attenuated inversion-recovery (hT2w-3D-FLAIR) (**A**: the thalamic level, **B**: the trigeminal nerve level) and diffusion tensor imaging (DTI) color maps (**C**: the thalamic level, **D**: the trigeminal nerve level) of a single patient are presented. The corticospinal tract (CST), medial lemniscus (ML), and superior cerebellar peduncle (SCP) are visualized as high-intensity areas on hT2w-3D-FLAIR images (**A**, **B**). These WM-tracts run through the following anatomical points on axial hT2w-3D-FLAIR: CST, 20 mm lateral from the lateral margin of the third ventricle (3<sup>rd</sup> V) at the thalamic level (point A on **A**); ML, 6 mm anterior to the anterior margin of the fourth ventricle (4<sup>th</sup> V) at the trigeminal nerve level (point B on **B**); and SCP, just lateral to the 4<sup>th</sup> V at the trigeminal nerve level (point C on **B**). The following WM-tracts run through these anatomical points on the axial DTI color maps: (point A on **C**) CST; (point B on **D**) ML; and (point C on **D**) SCP. The WM-tracts observed on hT2w-3D-FLAIR and DTI color maps completely correspond, and these WM-tracts are considered to be identical structures.

2D-FLAIR and 2D-T2-weighted imaging was recently reported.<sup>13)</sup> Compared with this previous report, the spatial resolutions of images in the present study were higher and had less distortion with the readout-segmented multi-shot EPI (RESOLVE)-based sequence used in the present study. In addition, the coronal and sagittal hT2w-3D-FLAIR images were reconstructed from axial images, and the hT2w-3D-FLAIR images in three directions were evaluated to investigate the continuity of the WM-tracts in the present study. On these points, the present study has several advantages compared with the previous report. The visibility of WM-tracts or the contrast between WM-tracts and the surrounding structures on hT2w-3D-FLAIR have the potential to surpass those on conventional 3D-FLAIR. These are the important comparative research issues that must be probed in future investigations.

The present study has some limitations. The effect of delayed enhancement cannot be excluded. The statistical comparison of plain and delayed enhanced images should be conducted in another investigation, although the principal purpose of this technical developmental study is to propound hT2w-3D-FLAIR as a potentially supplemental DTI neurographic modality. Furthermore, the results of the present study are chance findings in a protocol used clinically for inner ear investigation. Therefore, further potential protocol optimization for the purpose of visualization of WM-tracts should be established.

## CONCLUSION

In conclusion, the present study revealed that the CST, ML, and SCP were visualized on high-resolution hT2w-3D-FLAIR. hT2w-3D-FLAIR has the possibility of providing supplementary information to DTI.

## ACKNOWLEDGEMENTS

The authors would like to thank the radiological technologists of the MRI unit at our institute for their valuable contributions to the MRI examinations. In addition, the author also would like to express appreciation for Dr. Wataru Koike, Dr. Keiji Matsuo and Mrs. Naomi Yamazaki for their great support. This work was previously presented at the European Congress of Radiology (ECR) 2013, partially. This work was supported by grants from the Japan Society for the Promotion of Science (JSPS) for Masahiro Yamazaki (JSPS KAKENHI Grant Number 24791288) and Shinji Naganawa (JSPS KAKENHI Grant Number 22390233).

Conflict of Interest: None

## REFERENCES

- 1) Naganawa S, Kawai H, Sone M, Nakashima T. Increased sensitivity to low concentration gadolinium contrast by optimized heavily T2-weighted 3D-FLAIR to visualize endolymphatic space. *Magn Reson Med Sci*, 2010; 9: 73–80.
- 2) Naganawa S, Yamazaki M, Kawai H, Bokura K, Sone M, Nakashima T. Visualization of endolymphatic hydrops in Meniere's disease with single-dose intravenous gadolinium-based contrast media using heavily T2-weighted 3D-FLAIR. *Magn Reson Med Sci*, 2010; 9: 237–242.
- 3) Naganawa S, Komada T, Fukatsu H, Ishigaki T, Takizawa O. Observation of contrast enhancement in the cochlear fluid space of healthy subjects using a 3D-FLAIR sequence at 3 Tesla. *Eur Radiol*, 2006; 16:

## WM-TRACT VISUALIZATION BY HT2W-3D-FLAIR

- 733–737.
- 4) Griswold MA, Jakob PM, Heidemann RM, Nittka M, Jellus V, Wang J, Kiefer B, Haase A. Generalized autocalibrating partially parallel acquisitions (GRAPPA). *Magn Reson Med*, 2002; 47: 1202–1210.
  - 5) Porter DA, Heidemann RM. High resolution diffusion-weighted imaging using readout-segmented echo-planar imaging, parallel imaging and a two-dimensional navigator-based reacquisition. *Magn Reson Med*, 2009; 62: 468–475.
  - 6) De Coene B, Hajnal JV, Pennock JM, Bydder GM. MRI of the brain stem using fluid attenuated inversion recovery pulse sequences. *Neuroradiology*, 1993; 35: 327–331.
  - 7) Yagishita A, Nakano I, Oda M, Hirano A. Location of the corticospinal tract in the internal capsule at MR imaging. *Radiology*, 1994; 191: 455–460.
  - 8) Weigel M, Hennig J. Diffusion sensitivity of turbo spin echo sequences. *Magn Reson Med*, 2012; 67: 1528–1537.
  - 9) Adachi M, Kawanami T, Ohshima H, Hosoya T. Characteristic signal changes in the pontine base on T2- and multishot diffusion-weighted images in spinocerebellar ataxia type 1. *Neuroradiology*, 2006; 48: 8–13.
  - 10) Yasmin H, Aoki S, Abe O, Nakata Y, Hayashi N, Masutani Y, Goto M, Ohtomo K. Tract-specific analysis of white matter pathways in healthy subjects: a pilot study using diffusion tensor MRI. *Neuroradiology*, 2009; 51: 831–840.
  - 11) Takahara T, Hendrikse J, Kwee TC, Yamashita T, Van Cauteren M, Polders D, Boer V, Imai Y, Mali WP, Luijten PR. Diffusion-weighted MR neurography of the sacral plexus with unidirectional motion probing gradients. *Eur Radiol*, 2010; 20: 1221–1226.
  - 12) Naganawa S, Yamazaki M, Kawai H, Sone M, Nakashima T, Isoda H. Anatomical details of the brainstem and cranial nerves visualized by high resolution readout-segmented multi-shot echo-planar diffusion-weighted images using unidirectional MPG at 3T. *Magn Reson Med Sci*, 2011; 10: 269–275.
  - 13) Kitajima M, Hirai T, Shigematsu Y, Uetani H, Iwashita K, Morita K, Komi M, Yamashita Y. Comparison of 3D FLAIR, 2D FLAIR, and 2D T2-weighted MR imaging of brain stem anatomy. *AJNR Am J Neuroradiol*, 2012; 33: 922–927.